Cu decay into neutron-rich Zn isotopes: shell structure near ^{78}Ni

-

β-decay study of ^{75}Cu

Summer student project

Supervisors

Bruno Olaizola Mampaso

Andrés Illana Sisón

Student

Damiano Stramaccioni

October 2021

1 Introduction

1.1 Motivation

The Nuclear Shell Model represents a cornerstone in the study of the nuclear stability properties, in particular thanks to this model we are able to understand why for a certain set of protons and neutrons numbers (magic numbers) nuclei have greater binding energies compared to the near ones in the Segré Chart. The model allows accurate predictions along the valley of stability, while for exotic regions, as the neutron-drip line, the experiments performed have shown a rearrangement of the nuclear structure with the appearance of new magic numbers and the possible disappearance of the old ones [1]. Nickel isotopes have attracted a lot of attention in the last years due to their particular predisposition for the studies about the evolution of the nuclear stability as a function of the neutron-to-proton ratio. These nuclei are the only ones in the nuclide chart to have three different doubly-magic isotopes: the most neutron-deficient $^{48}_{20}Ni_{28}$, the one with the highest binding energy per nucleon $^{56}_{28}Ni_{28}$ and the most neutron-rich $^{78}_{50}Ni_{28}$. A great interest has developed on the $^{78}_{50}Ni_{28}$, for which a direct evidence of its doubly-magicity has recently been reported [2]. Other effects - as shape coexistence - were observed near this nucleus, even though the Nuclear Shell Model does not predict these phenomena to take place near doubly-magic nuclei. Since ^{78}Ni and the nuclei below cannot be reached using the present generation of ISOL facilities, the only way to get information about this zone is by studying the neighboring nuclei above it. The Zn isotopes, with only two protons above Ni and the increasing occupation of the neutron shell $1g_{9/2}$ represent a rich laboratory to study the evolution of the proton shell gap, Z=28, and the stability of the neutron shell gap, N=50, near the doubly-magic ^{78}Ni. Moreover the focus on this zone comes also from the crucial role that the magicity of N = 50, far from stability, plays in the rapid neutron-capture process in astrophysics.
This work analyses the level scheme of the ^{75}Zn, populated in the β-decay of ^{75}Cu.

1.2 Experimental setup

The experiment has been performed at the ISOLDE [3] facility in 2018 using the ISOLDE Decay Station (IDS) setup with four Clover HPGe detectors, two $LaBr_3$(Ce) detectors, a fast plastic detector and in combination with the tape station. The copper isotopes were produced in proton-induced fission reactions using a UC_x target at the ISOLDE facility in 2018. Subsequently, the isotopes were selectively ionized in the laser ion source, accelerated, mass separated, and sent to the experimental setup. In this case the neutron converter was essential in order to suppress the neutron-deficient contaminants, like Rb. Unfortunately, the isobaric contamination in the neutron-rich region, Ga in this case, was impossible to eliminate. However, the largest level of contamination expected was two orders of magnitude higher than the Cu beam intensity. This contamination was reduced adapting the beam-gate time, due to the different release from the UC_x target that each element has, and tape cycles depending of the half-lives of nuclei of interest and the isobaric contaminants [1].

2 Analysis

The first procedure followed was the energy and efficiency calibration performed with two radioactive source runs with ^{152}Eu and ^{133}Ba. Using the add-back algorithm an absolute efficiency $\sim 11\%$ was found at 200 keV and $\sim 2.6\%$ at 2 MeV. The add-back algorithm allows to recreate a full-energy event when a photon is scattered in two adjacent crystals.
The construction of a nuclear level scheme is based on the determination of energy, spin and parity of the levels involved in the γ-decays of the nucleus. During these decays, γ-rays in cascade are emitted in a quick sequence (i.e. in cascade), allowing the identification of the gamma rays involved through the analysis of coincidence measurements. Coincidence measurements allow to identify the γ-rays involved and the relative transitions; in addition they allow to discriminate γ-rays associated to the possible contaminants (mainly ^{75}Ga). The energy spectrum with all the γ identified in coincidence with β-particles was built using a coincidence window between -100 ns and 100 ns for β-γ events.
In order to find γ coincidences, a β-gated γ-γ coincidence matrix has been created. This matrix was filled with γ-γ coincidence condition nested in the γ-β coincidence one with the γ-γ window between -25 ns and 25 ns. β-γ gated spectra were obtained from gated projections of the β-γ-γ matrix, the background subtraction was made by subtracting normalized gated spectra outside the prompt window chosen for the peak. The intensities have been evaluated as the ratio between the number of photons associated to the transition and the efficiency (in add-back mode) at the corresponding energy. γ-rays directly feeding the ground state were identified comparing the single γ-spectrum with the coincidence matrix.
In the case of the 25 keV transition, since the electron conversion is expected to dominate the decay mode, the intensity of the gamma detected should not reflect the number of transitions between the 152 keV and the 127 keV levels. The number of coincidences between this gamma transition and other two gammas in the same cascade was analysed to obtain the branching ratio of the electron conversion process. In particular, being c this branching ratio, N_1 the number of coincidences of the 25 keV gamma with the first other gamma and N_2 the number of coincidences of the latter with a third gamma in the same cascade, we have:

$$[N_1(1-c)]/N_2 = k. \tag{1}$$

Since the expected value of N_1 and N_2 are $N_1 = \varepsilon(\gamma_1)\varepsilon(25)N$ and $N_2 = \varepsilon(\gamma_1)\varepsilon(\gamma_2)N$, with N the number of times the nucleus de-excited through this cascade in the experiment and ε(E) the efficiency of the γ-ray detector at the energy E, we can invert the formula (1) to obtain c. From this value the multipolarity of the transition can be inferred, along with the spin and parity of the 152 keV level:

$$c = 1 - k(\varepsilon(\gamma_2)/\varepsilon(25)) \quad \rightarrow c = 0.86(2) \quad \rightarrow \quad ICC = 5.9(8). \tag{2}$$

In particular, the value obtained for c allowed, using a conversion coefficient calculator [13], to establish the mixed E2 and M1 nature of this transition. The value deduced for the mixing ratio is δ=$0.17^{+0.2}_{-0.3}$, and results in the assignment of $\frac{3}{2}^-$ as the J^π value of the 152 keV level. Indeed, being $\frac{1}{2}^-$ the J^π for the 127 keV level [11], the deduced multipolarity of the transition restricts the possible values of J to (1/2 - 3/2), from M1, and to (3/2 - 5/2), from E2 - while the parity has to be negative. The intersection of the two intervals obtained allows the 152 keV level to have uniquely a J=$\frac{3}{2}$. For each level of the ^{75}Zn the relative β intensity has been derived from the difference between the (relative) intensities of the gamma-rays which arrive and leave the energy level, taking also into account the 3.5% branching ratio of the β neutron delayed emission process

[8].
The log(ft) values have been computed using a program set in NNDC [14], assuming the following parameters: $J^{\pi}(^{75}Cu)=\frac{5}{2}^{-}$ [5], $T_{1/2}$=1.224(3) s [8], Q(β^{-})=8088(3) keV [10], %β decay=96.5 [9]. All β-feedings should be treated as upper limits and associated log(ft) as lower limits.

3 Results

3.1 Energy levels

The γ-γ-β coincidence analysis allowed to expand the nuclear level scheme of the ^{75}Zn derived by S.V. Ilyushkin et al. [4]. Dashed lines identify uncertain transitions and levels. Curved brackets identify ranges of angular momentum.

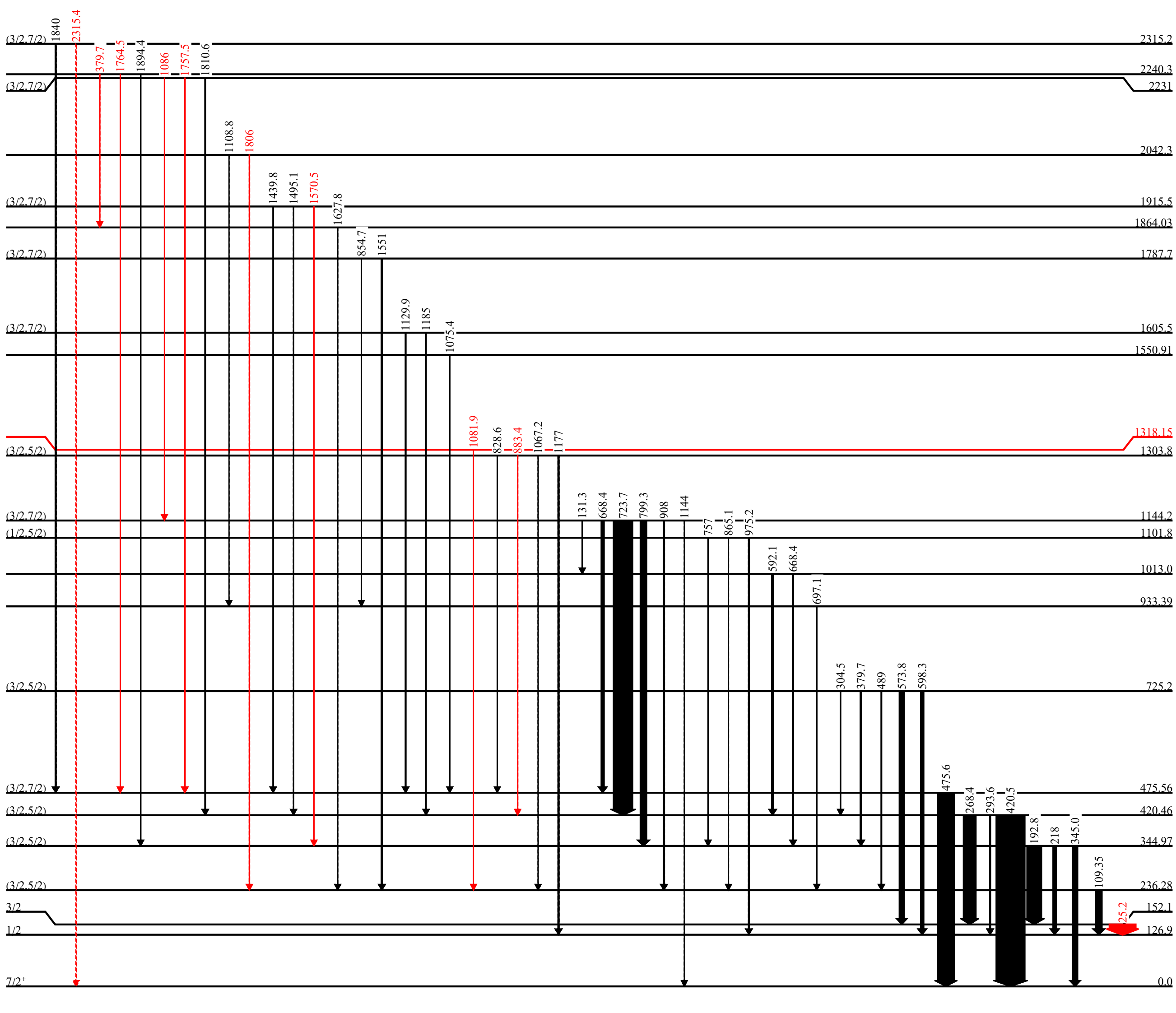

Figure 1: *Low energy portion of the nuclear level scheme derived for the ^{75}Zn. Already known levels and γ-rays are in black, while new ones are in red.*

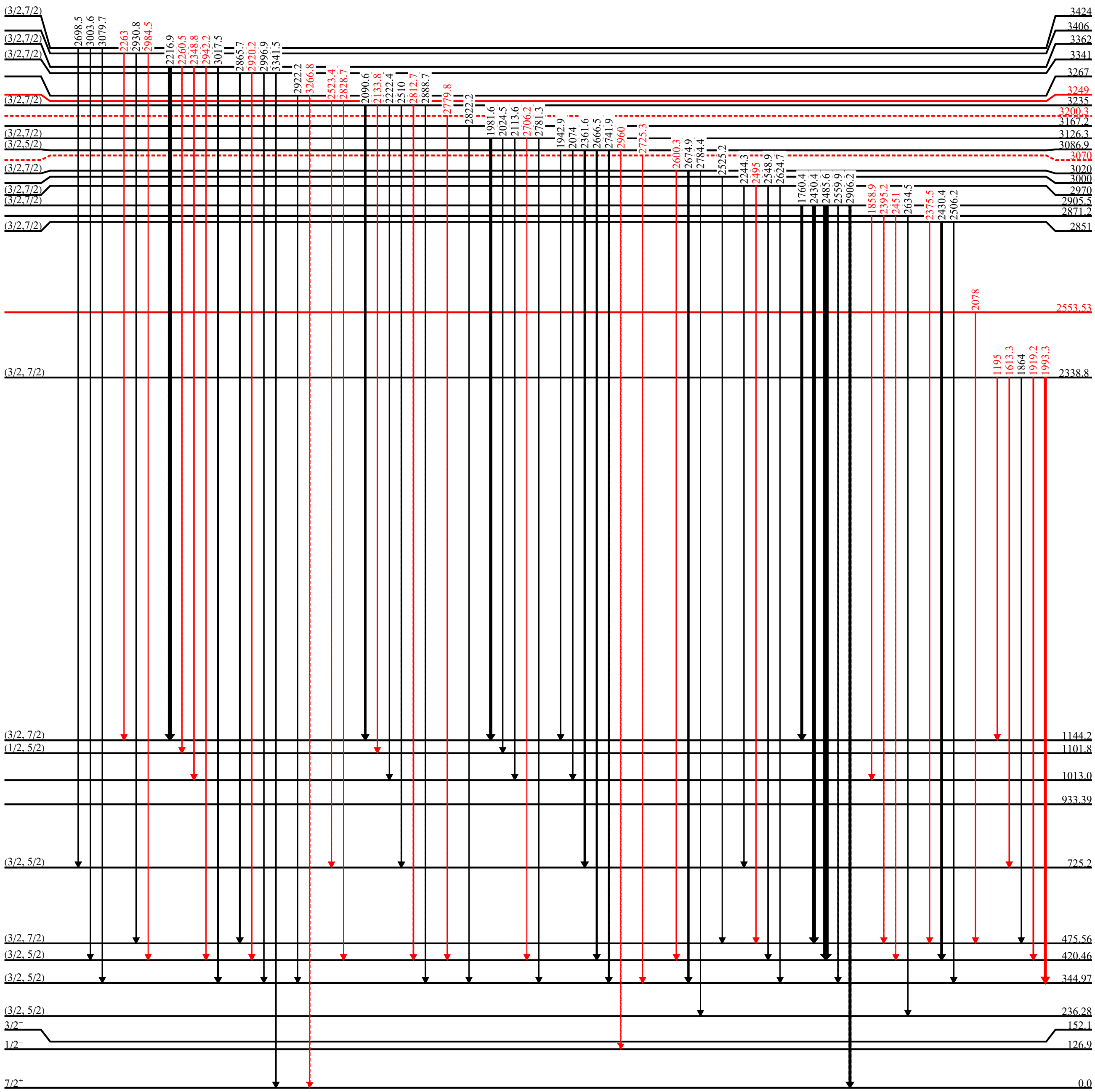

Figure 2: *Intermediate energy portion of the nuclear level scheme derived for the* ^{75}*Zn. Already known levels and* γ*-rays are in black, while new ones are in red.*

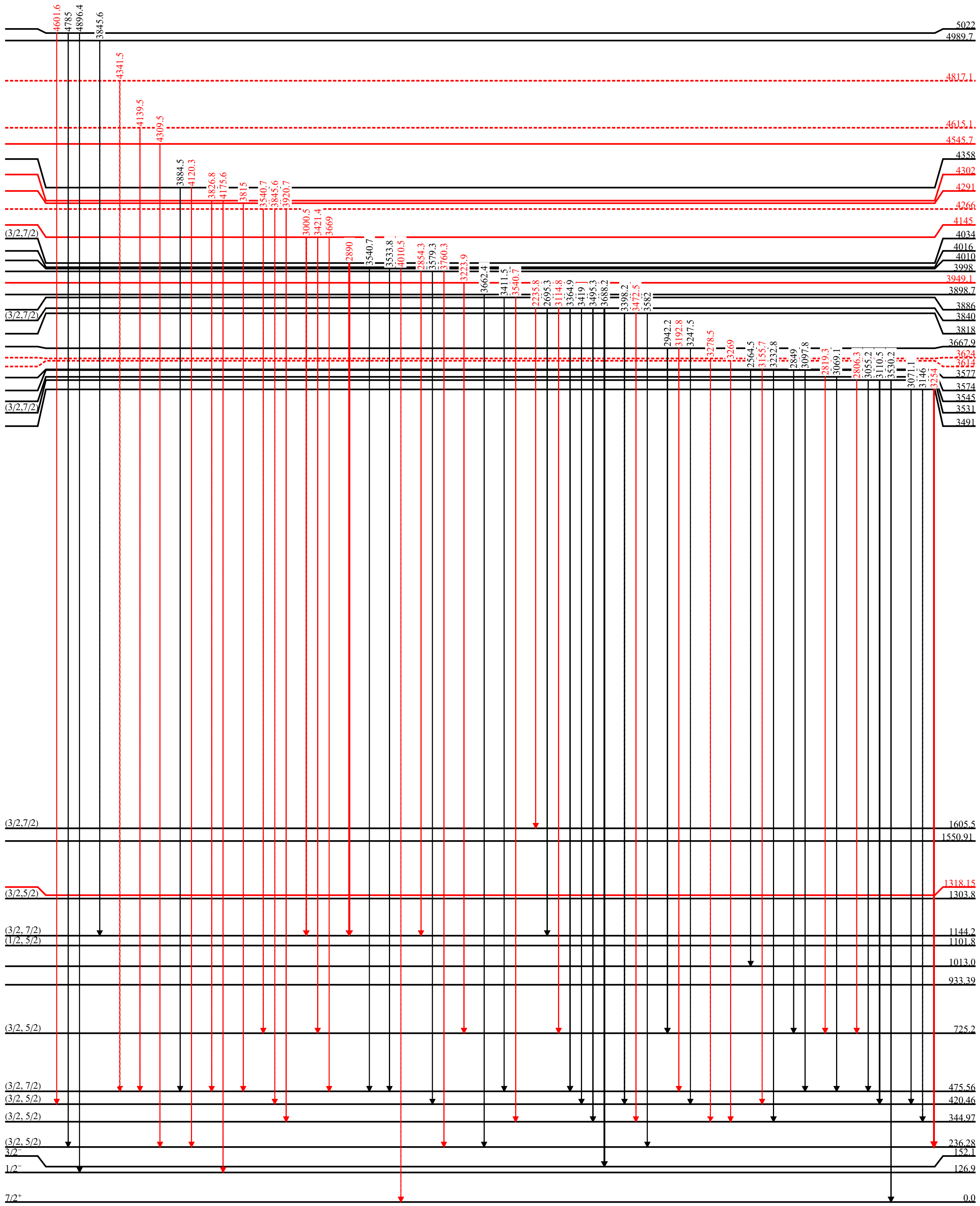

Figure 3: *High energy portion of the nuclear level scheme derived for the* ^{75}*Zn. Already known levels and* γ*-rays are in black, while new ones are in red.*

3.2 β-feeding

β-decay $^{75}Cu \rightarrow ^{75}Zn$ data regarding energy of the levels, β-feeding intensities and $\log(ft)$ values deduced in this work are shown below, along with the data reported in the previous work on this nucleus [4]. Curved brackets identify ranges of angular momentum.

Energy(keV)	**I$_\beta$(rel)**	**log(ft)**	**J$^\pi$**	**I$_\beta$(rel)$_{Lit}$ [4]**	**log(ft)$_{Lit}$ [4]**
236.28(5)	0.68(5)	7.15(3)	(1/2 - 5/2)		
344.97(5)	3.2(1)	6.47(1)	(3/2 - 5/2)	3.2(7)	6.47(10)
420.46(5)	5.0(6)	6.26(6)	(3/2 - 5/2)	5(1)	6.25(10)
475.56(5)	2.14(6)	6.61(1)	(3/2 - 9/2)	1.8(4)	6.69(10)
725.2(4)	4.74(4)	6.200(4)	(3/2 - 5/2)	2.1(4)	6.57(9)
933.39(5)	0.005(9)				
1013.0(3)	0.88(4)				
1101.8(4)	0.75(3)		(1/2 - 5/2)		
1144.2(2)	17.69(8)	5.511(2)	(3/2 - 7/2)	16.6(3.5)	5.53(11)
1303.8(3)	2.07(2)	6.396(5)	(3/2 - 5/2)		
1318.15(5)	0.04(1)				
1550.91(5)	0.306(9)				
1605.5(1)	1.25(2)	6.524(7)	(3/2 - 7/2)		
1787.7(4)	1.29(2)	6.454(7)	(3/2 - 7/2)		
1864.03(5)	0.04(1)				
1915.5(1)	1.20(2)	6.444(8)	(3/2 - 7/2)		
2042.3(1)	0.61(2)				
2231(1)	1.70(3)	6.189(8)	(3/2 - 7/2)		
2241.1(8)	0.978(2)				
2315.2(1)	1.70(3)	6.160(8)	(3/2 - 7/2)		
2338.8(8)	2.67(3)	5.958(5)	(3/2 - 7/2)		
2553.53(5)	0.24(1)				
2851.0(2)	2.60(3)	5.784(6)	(3/2 - 7/2)		
2905.5(7)	12.64(7)	5.076(3)	(3/2 - 7/2)	7.9(1.7)	5.29(9)
2969.8(4)	1.02(2)	6.15(1)	(3/2 - 7/2)		
3020.3(4)	2.75(4)	5.693(7)	(3/2 - 7/2)		
3086.9(2)	4.70(5)	5.436(5)	(3/2 - 5/2)		
3126.3(4)	3.15(4)	5.594(6)	(3/2 - 7/2)		
3235(1)	3.93(5)	5.455(6)	(3/2 - 7/2)		
3341.3(5)	1.90(3)	5.727(7)	(3/2 - 7/2)		
3362.0(6)	5.73(5)	5.239(4)	(3/2 - 7/2)		
3424.2(4)	1.06(3)	5.95(1)	(3/2 - 7/2)		
3530.8(5)	1.62(3)	5.717(9)	(3/2 - 7/2)		
3840.2(7)	2.44(4)	5.403(8)	(3/2 - 7/2)		
4034.2(1)	1.35(3)	5.57(1)	(3/2 - 7/2)		

Table 1: Energy, β-feeding intensities, angular momentum intervals and $\log(ft)$ values of the most relevant levels of ^{75}Zn deduced in this work, along with the corresponding β-feeding intensities and $\log(ft)$ values reported in the previous work on this nucleus [4].

The log(ft) values values were calculated only for the levels with I_β(rel)$\geq$1%, identified as the ones directly fed by ^{75}Cu. Apart from these levels, energy, β intensity and angular momentum interval were reported for all the identified levels with energy less than 3 MeV.

With the setup chosen for this experiment it was not possible to evaluate directly angular momentum of the energy levels by angular correlations analysis of the γ-ray transitions. However, as shown in the table above, from the lower levels it is however possible to evaluate the angular momentum intervals of the higher levels through the selection rules [12] with the restriction on the angular momentum of the transitions to values L $\leq$ 2 - as highlighted in the analysis of the β-decay data. This method was applied, for example, to the level 725 keV: from this level the nucleus decays γ to two levels of known J^π, namely 127 keV ($J^\pi = \frac{1}{2}^-$) and 152 keV ($J^\pi = \frac{3}{2}^-$). With the assumption L $\leq$ 2 for these transitions we may restrict the angular momentum of the level 725 keV to the interval (1/2 - 5/2). Considering then the log(ft) value deduced for this level, having the starting level of the β decay a J^π of $\frac{5}{2}^-$ [5], its angular momentum should belong to the (3/2 - 7/2) interval. The intersection of the two ranges is (3/2 - 5/2) which may include the angular momentum value of the level.

4 Conclusions

The analysis presented in this report has been successful in extending the level scheme of ^{75}Zn via the β decay of ^{75}Cu. In total, 15 new energy levels and 66 additional γ-rays to those found by S.V. Ilyushkin *et al.* [4] have been associated with this nucleus. Not all the γ-rays identified were placed in the scheme, generally due to the low statistics of the transitions. As it was mentioned before, the log (ft) values should be considered as lower limits due to the *Pandemonium* effect [6, 7]. Therefore, we may assume that the β-transitions are mainly at most first-forbidden unique.We were able to establish the spin and parity of the 152 keV level $J^\pi = \frac{3}{2}^-$ from the multipolarity deduced for the 25 keV γ transition to the 127 keV state, obtained through coincidences analysis. This is the first time the 25 keV γ ray was observed, since in the previous work about this nucleus [4] this energy was below the detection limit. Its observation firmly rules out that the 152 keV level is a β-decaying isomer, as was already hypothesized in [4]. As shown above, for the other levels it is sometimes possible to evaluate a range of angular momentum by the selections rules and the condition L $\leq$ 2 - but generally in order to determine these values a setup built for angular correlations study is necessary. Finally, as it can be appreciated from the table in the previous section, the angular momentum intervals deduced in this work are in agreement with the previous work on ^{75}Zn [4].

References

[1] Olaizola, B. and Illana, A. - IS622 Proposal *"Cu decay into neutron-rich Zn isotopes: shell structure near ^{78}Ni"* (2016). https://cds.cern.ch/record/2717898/files/INTC-P-554.pdf

[2] Taniuchi, R. *et al.*, Nature **569** 53–58 (2019).

[3] Borge, M.J.G., Nucl. Instr. and Meth. B, **376**, 408-412 (2016).

[4] Ilyushkin, S.V. *et al.*, Phys. Rev. C, **83**, 014322 (2011).

[5] Flanagan, K. T. *et al.*, Phys. Rev. C, **103**, 142501 (2009).

[6] Rubio B. and Gelletly W., Beta Decay of Exotic Nuclei. In: Al-Khalili J., Roeckl E. (eds) The Euroschool Lectures on Physics with Exotic Beams, Vol. III. Lecture Notes in Physics, **764**. Springer, Berlin, Heidelberg (2009).

[7] Algora, A. *et al.*, Eur. Phys. J. A, **57** 85 (2021).

[8] Kameda, D. *et al.*, Phys. Rev. C, **86**, 054319 (2012).

[9] Reeder, P.L. *et al.*, Phys. Rev. C, **31**, 1029 (1985).

[10] Wang, M. *et al.*, Chin.Phys.C, **36**, 1603 (2012).

[11] Wraith, C. *et al.*, Phys. Lett. B, **771**,385-391 (2017).

[12] B. Singh *et al.*, Nuclear Data Sheets, **84**, 487 (1998).

[13] https://bricc.anu.edu.au/

[14] https://www.nndc.bnl.gov/logft/